Forward and backward Terahertz-wave difference-frequency generations from periodically poled lithium niobate

T. D. Wang[1], S. T. Lin[1], Y. Y. Lin[1], A. C. Chiang[2], and Y. C. Huang[1]

[1]*Institute of Photonics Technologies, Department of Electrical Engineering, National Tsing-hua University, Hsinchu 30013, Taiwan*

[2]*Nuclear Science and Technology Development Center, National Tsing-hua University, Hsinchu 30013, Taiwan*

ychuang@ee.nthu.edu.tw

Abstract: We report terahertz-wave generation in the wavelength range of 190~210 and 457~507 μm from forward and backward difference frequency generations, respectively, in a 3.2-cm long multi-grating periodically poled lithium niobate (PPLN) crystal. The grating period of the PPLN crystal varies form 63 to 70 μm in 1-μm increments. The extraordinary refractive index of lithium niobate in the THz-wave range was precisely deduced from the quasi-phase-matching condition of the difference frequency generations.

OCIS codes: (190.2620) Nonlinear Optics, frequency conversion; (190.4410) Nonlinear Optics, parametric processes.

References and links

1. C. Rønne, P. Åstrand, and S. R. Keiding, "THz spectroscopy of liquid H_2O and D_2O," Phys. Rev. Lett. **82**, 2888-2891 (1999).
2. E. Knoesel, M. Bonn, J. Shan, and T. F. Heinz, "Charge transport and carrier dynamics in liquids probed by THz Time-Domain Spectroscopy," Phys. Rev. Lett. **86**, 340-343 (2001).
3. K. Kawase, Y. Ogawa, Y. Watanabe, and H. Inoue, "Non-destructive terahertz imaging of illicit drugs using spectral fringeprints," Opt. Express. **11**, 2549-2554 (2003).
4. Q. Wu, T. D. Hewitt, and X.-C. Zhang, "Two-dimensional electro-optic imaging of THz beams," Appl. Phys. Lett. **69**, 1026-1028 (1996).
5. P. R. Smith, D. H. Auston, and M. C. Nuss, "Subpicosecond photoconducting dipole antennas," IEEE J. Quantum Electron. **24**, 255-256 (1988).
6. X.-C., B. B. Hu, J. T. Darrow, and D. H. Auston, "Generation of femtosecond electromagnetic pulses from semiconductor surface," Appl. Phys. Lett. **56,** 1011-1013 (1990).
7. D. H. Levy, *Free Electron Lasers and Other Advanced Sources of Light*, (National Academy Press Washington, DC, 1994) 24–31.
8. R. Köhler, A. Tredicucci, F. Beltram, H. E. Beere, E. H. Linfield, A. G. Davies, D. A. Ritchie, R. C. Iotti and F. Rossi, "Terahertz semiconductor-hetrostructure laser," Nature **417,** 156-159 (2002).
9. M. A. Piestrup, R. N. Fleming, and R. H. Pantell, "Continuously tunable submillimeter wave source," Appl. Phys. Lett. **26**, 418-419 (1975).
10. K. Kawase, M. Sato, T. Taniuchi, and H. Ito, "Coherent THz-wave generation from $LiNbO_3$ with monolithic grating coupler," Appl. Phy. Lett. **68**, 2483-2485 (1996).
11. J. Shikata, M. Sato, T. Taniuchi, and H. Ito, "Enhancement of Terahertz-wave output from $LiNbO_3$ optical parametric oscillator by cryogenic cooling," Opt. Lett. **24**, 202-204 (1999).
12. K. Kawase, J. Shikata, H. Minamide, K. Imai, and H. Ito, "Arrayed silicon prism coupler for THz-wave parametric oscillator," Appl. Opt. **40**, 1423-1426 (2001).
13. J. A. Armstrong, N. Bloemergen, J. Ducuing, and P. S. Pershan, "Interactions between light waves in a nonlinear dielectric," Phys. Rev. **127**, 1918-1939 (1962).
14. Y. S. Lee, T. Meade, V. Perlin, H. Winful, T. B. Norris, and A. Galvanauskas, "Generation of narrow-band terahertz radiation via optical rectification of femtosecond pulses in periodically poled lithium niobate," Appl. Phys. Lett. **78**, 2505-2507 (2000).
15. C. Weiss, G. Torosyan, J. P. Meyn, R. Wallenstein, R. Beigang, and Y. Avetisyan, "Tuning characteristics of narrowband THz radiation generated via optical rectification in periodically poled lithium niobate," Opt. Express **8,** 497-502 (2001).
16. N. E. Yu, C. Jung, C. S. Kee, Y. L. Lee, B. A. Yu, D. K. Ko, and J. Lee, "Backward terahertz generation in periodically poled lithium niobate crystal via difference frequency generation," Jpn. J. Appl. Phys. **46,** 1501-1504 (2007).

#94351 - $15.00 USD Received 27 Mar 2008; revised 18 Apr 2008; accepted 18 Apr 2008; published 22 Apr 2008

17. K. L. Vodopyanov, "Optical generation of narrow-band terahertz packets in periodically-inverted electro-optic crystals: conversion efficiency and optimal laser pulse format," Opt. Express **14,** 2263-2276 (2006).
18. W. Shi, Y. J. Ding, N. Fernelius, and K. Vodopyanov, "Efficient, tunable, and coherent 0.18-5.27-THz source based on GaSe crystal," Opt. Lett. **27**, 1454-1456 (2002).
19. Y. J. Ding and J. B. Khurgin, "A new scheme for efficient generation of coherent and incoherent submillimeter to THz wave in periodically-poled lithium niobate," Opt. Commun. **148**, 105-109 (1998).
20. S. E. Harris, "Proposed Backward Wave Oscillation in the Infrared," Appl. Phys. Lett. **9**, 114-115 (1966).
21. C. Canalias and V. Pasiskevicius, "Mirror-less optical parametric oscillator," Nat. Photonics **1**, 459-462 (2007).
22. W. Shi, and Y. J. Ding, "Backward parametric oscillation in second-order nonlinear medium," in *Conference on Lasers and Electro-Optics/Quantum Electronics and Laser Science and Photonic Applications Systems Technologies*, Technical Digest (CD) (Optical Society of America, 2005), paper QTuF7.
23. V. B. Podobedov, D. F. Plusquellic, and G. T. Fraser, "Investigation of the water-vapor continuum in the THz region using a multipass cell," J. Quant. Spectrosc. Radiat. Transfer **91**, 287-295(2005).
24. L. Pálfalvi, J. Hebling, J. Kuhl, Á. Péter and K. Polgár, "Temperature dependence of the absorption and refraction of Mg-doped congruent and stoichiometric $LiNbO_3$ in the THz range," J. Appl. Phys. **97**, 123505-123511 (2005).
25. E. D. Palik, *Handbook of Optical Constants of Solids*, 695-702 (Academic, New York, 1991).

1. Introduction

A terahertz (THz) wave source could be useful for applications such as spectroscopy, noninvasive imaging, and drug detection [1-4]. For incoherent THz radiation, ultra-fast laser gated optical rectification [5] and photoconductive switching [6] are two widely adopted schemes. For coherent THz radiation, there are also a number of approaches. For example, a free electron laser is capable of generating high-power and broadly tunable THz radiation [7]; however, its large size and high cost have restricted its use to a limited number of researchers. The THz quantum-cascade laser [8] is another type of coherent THz source, but room-temperature, high-power operation of such a source is not yet demonstrated. Optical parametric down conversion has been a popular scheme for generating coherent THz waves at room temperature. For example, THz-wave generation from polariton scatting in lithium niobate ($LiNbO_3$), pioneered by Pantell [9], has been greatly improved by Ito [10-12] in the past 10 years. With the non-collinear phase matching condition, the THz wave in $LiNbO_3$ is emitted at about 65° from the pump-beam direction and is often trapped inside the crystal due to the total internal reflection. Specially arranged Si prisms or gratings have been used to couple out the THz power from the $LiNbO_3$ crystal [12].

Usually, collinear phase-matching is the preferred configuration for a nonlinear frequency conversion process, because it provides the longest interaction length and more efficient power extraction from a normal-incidence crystal face. Optical rectification using a fs pump laser in a quasi-phase-matched (QPM) [13] nonlinear optical material can also generate forward and backward multi-cycle THz radiations [14-16]. The mechanism of the THz-wave generation is understood as a special case of difference frequency generation in that two Fourier components of the fs laser pulse perform wave mixing [17]. However in the collinear configuration the generated THz-wave quickly walks away from the short pump pulse and is mostly absorbed before existing the nonlinear optical material. On the other hand, the conventional collinearly phase-matched difference frequency generation using two coherent long-pulse pump components promises much more power and better coherence for the generated THz wave [18].

Previous theoretical studies [17, 19] have shown that both forward and backward difference frequency generations for THz waves can be conveniently arranged with a collinearly phase matched configuration in periodically pole lithium niobate (PPLN). The backward scheme is particular interesting in that mirror-less oscillation can be achieved with a sufficiently large pump intensity [20]. It is hoped that successful demonstration in the mid-infrared spectrum [21] could be extended to the THz-radiation spectrum. However, a THz backward optical parametric oscillator (OPO) would have a much higher pump threshold due to the relatively strong absorption and diffraction of the THz wave in a nonlinear optical material. Nonetheless, backward difference frequency generation of THz waves was demonstrated in a birefringence-phase-matched GaSe crystal [22]. Quasi-phase-matched

#94351 - $15.00 USD Received 27 Mar 2008; revised 18 Apr 2008; accepted 18 Apr 2008; published 22 Apr 2008

GaAs could be a good candidate for demonstrating a THz backward OPO, but the technique for fabricating a large-aperture, low-loss, long enough QPM GaAs is not yet available. In this paper, we demonstrate, to the best of our knowledge, the first forward and backward difference frequency generations of coherent THz waves from a multi-grating PPLN crystal. From the quasi-phase-matching condition, we precisely deduced the refractive index of $LiNbO_3$ in the THz spectrum.

2. Experimental setup

Figure 1 shows the experimental setup of the forward and backward THz difference frequency generations. A kHz-linewidth distributed-feedback diode laser (DFBDL) at 1538.98 nm and a MHz-linewidth external-cavity diode laser (ECDL) tunable between 1510 and 1610 nm provide the seed components to the first-stage Erbium-doped fiber amplifier (EDFA) and the second-stage pulsed optical parametric amplifier (OPA) for the THz difference frequency generations in the PPLN difference frequency generator (PPLN DFG). The EDFA boosts up the CW diode-laser powers to about 70 mW. A passively Q-switched Nd:YAG laser at 1064 nm pumps the OPA using a PPLN crystal as the gain medium. The PPLN-OPA crystal has a 0.78-mm thickness, 45-mm length, and 29.6-μm QPM period. The OPA pump laser generates 70-μJ pulse energy in a 500-ps pulse width repeating at a 1 kHz rate. The pump laser is focused to a waist radius of 166 μm at the center of the PPLN-OPA crystal. At 101°C, the PPLN OPA has a 12-nm or 1.6-THz bandwidth so this OPA can simultaneously amplify the two seed components from the diode lasers. After the OPA, each of the two seed components is amplified to ~8.5-μJ pulse energy in a 400-ps pulse width for pumping the THz PPLN DFG. The one-to-one power ratio in the two pump components maximizes the output power of the difference frequency generation in the low-conversion limit. The two idler waves of the OPA near 3.3 μm were completely absorbed by the BK7 substrate of the dichroic mirror (HR @1064 nm and HT @1550 nm). The two pump components near 1.5 μm were focused by a f = 7.5-cm focusing lens to a 130 μm waist radius at the center of a multi-grating PPLN-DFG crystal for performing the forward and backward THz difference frequency generations. One major advantage of this broadband two-stage amplifier system is that the spatial and temporal overlap of the two pump components of the PPLN DFG is automatically achieved. In addition, the THz frequency can be easily tuned by varying the relative frequency between the two seed diode lasers. The 400-ps pulse width of the OPA output, however, gives a walkoff distance between the optical and THz pulses comparable to the 3.2-cm crystal length of the PPLN DFG.

The DFG employed a multi-grating PPLN crystal with a 0.78-mm thickness. The PPLN crystal consists of 8 parallel QPM gratings with 63, 64, 65, 66, 67, 68, 69, and 70-μm domain periods. The end faces of the PPLN crystal were coated with anti-reflection dielectric layers at the two pump wavelengths (Reflectance <0.5%).

The forward THz wave was largely separated from the pump components by using a wire mesh in the down stream of the PPLN DFG. The wire mesh contains 45 μm × 45 μm square apertures with a 54% filling factor. The transmittance of the wire mesh is 14% and 84% for incident waves near 200 and 1.55 μm, respectively. The residual pump laser reflected from the wire mesh is completely blocked by a 3-mm thick Ge filter and a high-density polyethylene filter in front of the bolometer. The backward THz wave was extracted by using an optically polished 3.5 cm × 3.5 cm square copper reflector placed 3 cm in front of the multi-grating PPLN crystal. The copper reflector has a 5-mm diameter hole for transmitting the two pump components, but reflects nearly 94% of the THz wave incident on it. The counter-propagating configuration of the pump and THz waves in the backward THz-wave DFG provides a pump-free background for measuring the THz wave. When taking data, we scanned the wavelength of the ECDL and read the THz-wave signal from a 4K Si bolometer. When the ECDL wavelength is tuned to the quasi-phase-matching condition of the forward or backward difference frequency generation, the bolometer registers a large THz-wave signal. The bolometer signal fell back to the noise level when we blocked any of the two pump

#94351 - $15.00 USD Received 27 Mar 2008; revised 18 Apr 2008; accepted 18 Apr 2008; published 22 Apr 2008

components, so generation of the forward and backward THz waves was unambiguously confirmed.

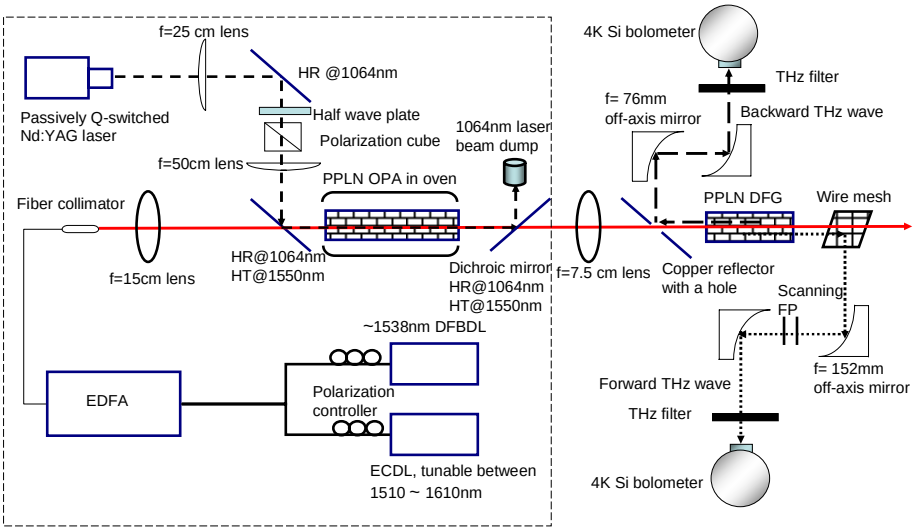

Fig. 1. Setup of the collinearly quasi-phase-matched forward and backward THz difference frequency generations in a multi-grating PPLN crystal. The two-stage amplifier, marked by a dashed-line box, generates 17-μJ pump energy in a 400-ps pulse width with two frequency components from the seeding DFBDL and the ECDL. The 17-μJ pump energy is injected to into the PPLN DFG for generating coherent THz radiation. The frequency tuning of the THz wave is achieved by varying the frequency difference between the two diode lasers matched to the QPM conditions of the DFG PPLN. (HR: high reflection, HT: high transmission, OPA: optical parametric amplifier, DFG: difference frequency generator, FP: Fabry-Perot spectrometer, ECDL: external-cavity diode laser, DFBDL: distributed-feedback diode laser, EDFA: Erbium-doped fiber amplifier.)

3. Experimental results

It can be shown from the plane-wave model that the phase-tuning curve of a highly lossy forward or backward THz-wave DFG has a Lorentzian line shape given by

$$I_{THz} \propto \left| j\Delta kL + \frac{\alpha_{THz}}{2} L \right|^{-2}, \tag{1}$$

where I_{THz} is the intensity of the THz wave, Δk is the wave-vector mismatch, L is the length of the nonlinear material, α_{THz} is the power attenuation coefficient at THz frequencies, and $j = \sqrt{-1}$ is the imaginary unit. Figure 2 shows the forward THz phase-tuning curves measured by the bolometer. The solid curves are the best fits of the Lorentzian function in Eq. (1). We deduced the phase-matched wavelength of the THz radiation λ_{THz} from the frequency conservation law, $1/\lambda_p - 1/\lambda_s = 1/\lambda_{THz}$, where λ_p and λ_s are the long- and short-wavelength pump components for the DFG, respectively. In Fig. 2(a), the phase-matched THz-radiation wavelengths were found to be 191.6, 194.4, 197.1, 199.6, 202.4, 205.0, and 206.8 μm, corresponding to the PPLN grating periods of 63, 64, 65, 66, 67, 68, and 69 μm, respectively. The best signal-to-noise ratio in the tuning curves is more than 10. The measurements were done in a laboratory atmosphere without dry-N_2 purge. As shown by Fig. 2(b), the THz wave generated from the 70-μm grating near 211.5 μm was strongly absorbed by the ambient water vapor [23]. We also verified the THz radiation by directly measuring its wavelength using a scanning Fabry-Perot spectrometer. The spectrometer consists of two parallel pieces of the wire mesh with a 2.5-μm scanning step along the longitudinal direction. A THz-radiation

#94351 - $15.00 USD Received 27 Mar 2008; revised 18 Apr 2008; accepted 18 Apr 2008; published 22 Apr 2008

wavelength of 197.5 μm was confirmed at the output of the 65-μm period PPLN, which is in good agreement with the wavelength deduced from the frequency conservation law.

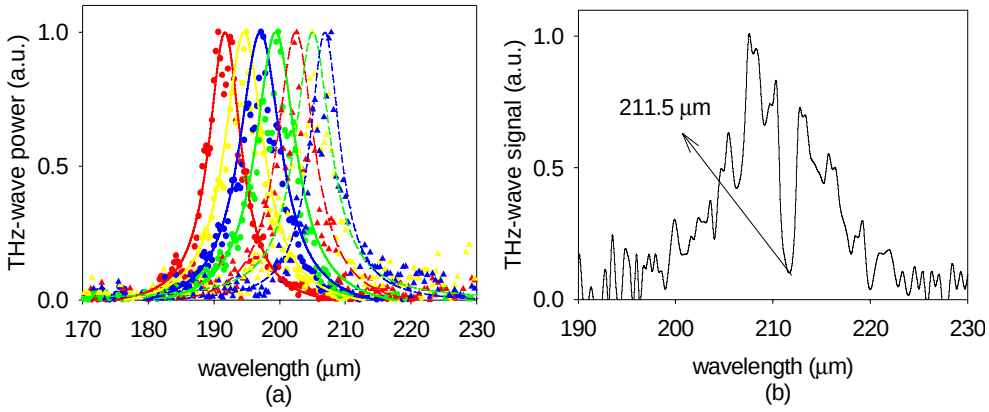

Fig. 2. (a). Forward THz-wave phase-matching curves measured by the 4K Si bolometer for the PPLN gratings with 63, 64, 65, 66, 67, 68 and 69-μm periods. The solid curves are the best fits of the Lorentzian function in Eq. (1). (b) When taking the phase matching cure for the 70-μm period PPLN DFG, we found absorption of ambient water vapor near 211.5 μm [23].

The bolometer was specified with 100% quantum efficiency at 200 μm. From the bolometer signal, we estimated about 10-fJ THz-wave energy entering the detection cone of the bolometer. Considering the 54, 35, 72% transmittances at PPLN output face, the Ge filter, and the bolometer window, respectively, and the fast diffraction of the THz, we obtain 0.37 pJ energy of THz radiation inside the PPLN crystal.

While fixing the wavelength of the DFBDL at 1538.43 nm, we continued to scan the ECDL wavelength and read the backward THz-wave signal from the 4K Si bolometer. In Fig. 3, we plot the backward DFG tuning curves measured by the bolometer. The phase-matched THz-radiation wavelengths were found to be 456.7, 463.8, 470.2, 477.7, 484.6, 492.6, 498.8, and 507.3 μm, corresponding to the PPLN grating periods of 63, 64, 65, 66, 67, 68, 69, and 70 μm, respectively. The measurements were also done in a laboratory atmosphere without dry-N_2 purge. For those measurements, the best signal-to-noise ratio in the tuning curves is also about 10.

In this experiment, the pump power for the backward THz DFG was about 2-3 orders of magnitudes lower than that for most THz-wave forward difference frequency generation in $LiNbO_3$. By assuming 100% quantum efficiency of our Si bolometer for the backward THz photons between 450~500 μm, we estimate ~6 fJ energy of the backward THz wave entering the detection cone of the bolometer. The backward THz wave was emitted from the input face of the PPLN crystal with a radiation area approximately equal to the pump laser area. Since the 130-μm pump laser radius is several times less than the radiation wavelength, the THz wave appears to radiate from a point source from the PPLN end face covering a nearly 2π solid angle. The first f = 76-mm, 2″-aperture off-axis parabolic mirror was responsible for collecting the THz radiation into the bolometer, which was placed ~7 cm from the PPLN input face due to the space constraint in our setup. This suggests that, with our current setup, only a very small fraction of the THz-wave energy collected into the sensor area of the bolometer. Further taking into account the ~50% Fresnel reflection at the PPLN surface, we conclude a minimum of 56-fJ energy of the backward THz wave was generated in the PPLN. Further improvements on the detection scheme and the detector calibration are needed to understand the conversion efficiency of this backward THz difference frequency generation. In addition, the short 400-ps pump pulse lengths only allow 200-ps buildup time for the backward-propagating THz wave in the highly absorptive PPLN. This means the effective gain length of our backward THz DFG is only 1.2 cm, given a THz refractive index of ~5.

#94351 - $15.00 USD Received 27 Mar 2008; revised 18 Apr 2008; accepted 18 Apr 2008; published 22 Apr 2008

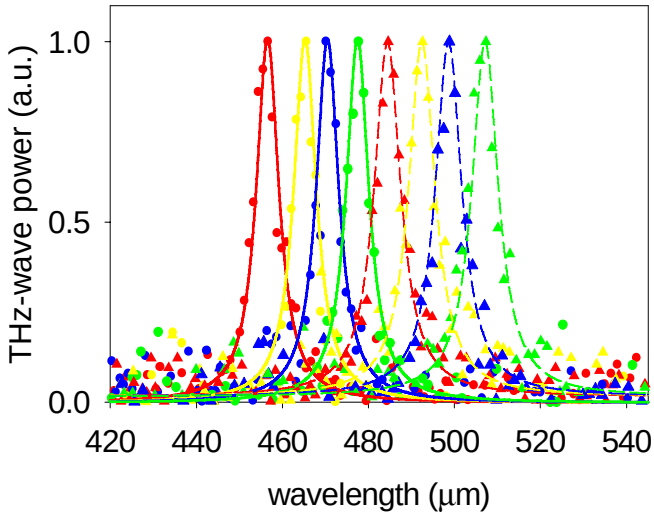

Fig. 3. Backward THz-wave phase matching curves measured by the 4K Si bolometer for the PPLN with 63, 64, 65, 66, 67, 68, 69 and 70-μm periods. The solid curves are the best fits of the Lorentzian function in Eq. (1).

Table 1 summaries the generated THz wavelengths and deduced refractive indices of the forward and backward THz difference frequency generations. For the forward THz-wave generation, the data for the 70-μm PPLN grating period is not available (NA) due to water absorption at the generated wavelength. The refractive index can be deduced from the QPM condition $n_p/\lambda_p - n_s/\lambda_s - 1/\Lambda_{PPLN} = \pm n_{THz}/\lambda_{THz}$ with known material dispersion at the optical frequencies, where the + and – signs denote the forward and backward processes, respectively, Λ_{PPLN} is the PPLN grating period, and n is the refractive index. For the PPLN DFG, n_{THz} is the extraordinary refractive index seen by the THz radiation.

Table 1. Summary of the forward and backward THz difference frequency generations

Forward THz-wave Generation								
PPLN period (μm)	63	64	65	66	67	68	69	70
Measured THz wavelength (μm)	191.6	194.4	197.1	199.6	202.4	205.0	206.8	NA
Deduced extraordinary refractive index	5.2243	5.2203	5.2152	5.2064	5.2039	5.1976	5.1794	NA
Backward THz-wave Generation								
Measured THz wavelength (μm)	456.7	463.8	470.2	477.7	484.6	492.6	498.8	507.3
Deduced extraordinary refractive index	5.0663	5.0641	5.0512	5.0559	5.0494	5.0609	5.0456	5.0638

#94351 - $15.00 USD Received 27 Mar 2008; revised 18 Apr 2008; accepted 18 Apr 2008; published 22 Apr 2008

Figures 4(a) and 4(b) show the measured extraordinary refractive indices (dots) versus the forward and backward THz-wave wavelengths, respectively. For comparison, we also overlay on the same plots the fitting curves of the THz-wave refractive index from Refs. [24, 25]. In Fig. 4(a), the fitting curve from Ref. [24] matches reasonably well to our measured data. In Fig. 4(b), the experimental data are in a good agreement with Ref. [25]. Usually it is relatively difficult to precisely measure the refractive index of a material at the THz frequency. The quasi-phase-matched difference generations offer a convenient and precise way of characterizing material dispersion at THz frequencies.

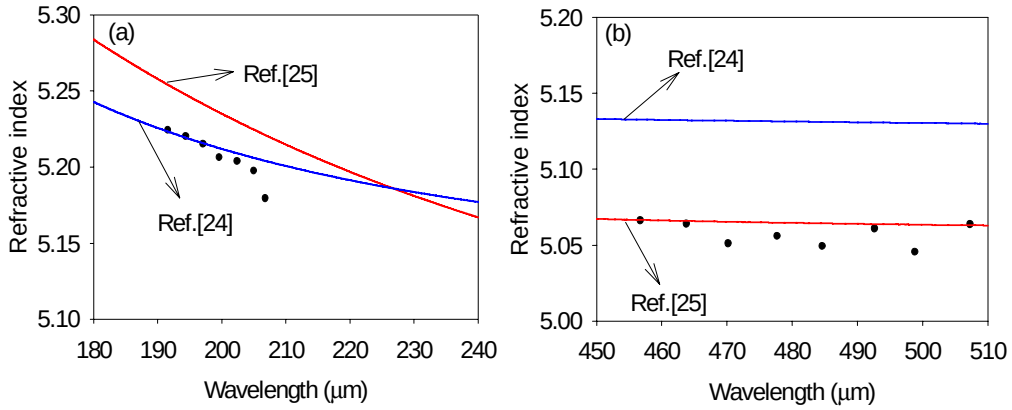

Fig. 4. The THz extraordinary refractive indices deduced from the (a) forward and (b) backward THz-wave difference frequency generations. The fitting curves from Refs. [24, 25] are also shown for comparison.

4. Discussion and conclusion

Although the QPM technique holds some promise to increase the gain length for parametric THz-wave generation from $LiNbO_3$, future work is necessary to make a direct comparison between the collinear and non-collinear phase-matching schemes under the same pump power and radiation wavelength. As an attempt to achieve backward parametric oscillation, we also used a single high-power source to pump the PPLN crystal but only generated high-order phase-matched forward mid-infrared radiation. Apparently, in our PPLN crystal, the net gain of the backward parametric process for THz-wave generation is much lower than that of the forward parametric process for mid-infrared generation. Forced nonlinear dipole radiation with a more intense seed signal for the DFG could be an approach to achieve backward-wave oscillation at the THz frequencies.

We have demonstrated collinearly quasi-phase-matched forward and backward DFG for generating THz waves near 200 and 500 μm, respectively, from a multi-grating PPLN crystal with a pump power 2~3 orders of magnitude lower than that for most THz-wave generations using $LiNbO_3$. Owing to the narrow linewidths of the two seed diode lasers, the generated THz waves are expected to be transform limited. We estimated that about 0.37 and 0.056 pJ energies of the forward and backward THz waves, respectively, were generated in the PPLN crystal. Owing to the vast difference in the optical and THz refractive indices in $LiNbO_3$, the 400-ps pump pulse width could have limited the effective gain lengths for both the forward and backward DFG's. We also found from a plane-wave model that the ideal power ratio for the two pump powers deviated from the one-to-one ratio in a pump-depleted, high-gain DFG. We expect to generate much more THz-wave energy by using more intense pump sources with a longer pulse length and a more optimized power ratio in our future work. Further improvements on collecting the quickly diffracted THz wave and calibrating the THz detector are among our next efforts for understanding and maximizing the efficiency of the THz difference frequency generations. Nonetheless, the QPM forward and backward difference frequency generations are very effective for measuring the refractive index of $LiNbO_3$ at the

#94351 - $15.00 USD Received 27 Mar 2008; revised 18 Apr 2008; accepted 18 Apr 2008; published 22 Apr 2008

THz frequencies. What has been accomplished in this work is potentially an important step toward the realization of a tunable, low-pump-power coherent THz source.

Acknowledgments

We appreciate some fruitful discussion with Fan-Yi Lin. This work was supported by the National Science Council of Taiwan under Contract NSC 95-2112-M-007-027-MY2.
Y. C. Huang's e-mail address is ychuang@ee.nthu.edu.tw.

#94351 - $15.00 USD Received 27 Mar 2008; revised 18 Apr 2008; accepted 18 Apr 2008; published 22 Apr 2008